

Durham Research Online

Deposited in DRO:

17 November 2017

Version of attached file:

Accepted Version

Peer-review status of attached file:

Peer-reviewed

Citation for published item:

Perrin, Andrea and Goodwin, Melissa J. and Musa, Osama M. and Yufit, Dimitrii S and Steed, Jonathan W. (2017) 'Boric acid co-crystals in guar gelation.', CrystEngComm., 19 (47). pp. 7125-7131.

Further information on publisher's website:

<https://doi.org/10.1039/C7CE01858D>

Publisher's copyright statement:

Additional information:

Use policy

The full-text may be used and/or reproduced, and given to third parties in any format or medium, without prior permission or charge, for personal research or study, educational, or not-for-profit purposes provided that:

- a full bibliographic reference is made to the original source
- a [link](#) is made to the metadata record in DRO
- the full-text is not changed in any way

The full-text must not be sold in any format or medium without the formal permission of the copyright holders.

Please consult the [full DRO policy](#) for further details.

Received 00th January 20xx,

Boric Acid Co-crystals in Guar Gelation

 Andrea Perrin,^a Melissa J. Goodwin,^a Osama M. Musa,^b Dmitry S. Yufit^a and Jonathan W. Steed^{a*}

Accepted 00th January 20xx

DOI: 10.1039/x0xx00000x

www.rsc.org/

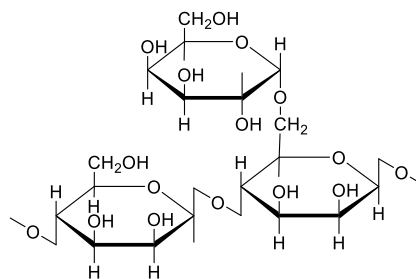
A series of bis(pyrrolidone) and ϵ -caprolactam co-crystals of boric acid and 1,4-phenylenediboric acid are reported. The high polarity of the lactam carbonyl group is highly complementary to the boronic acid hydrogen bond donor functionalities and co-crystals are based on cyclic boronic acid tape motifs, including an unusual donor-donor motif, with strong perpendicular interactions to the lactam functionalities. All of the co-crystals are able to act as a source of boric or boronic acid cross-linker in guar gelation.

Introduction

The strong hydrogen bond donor ability and relatively weak hydrogen bond acceptance of boric acid and its derivatives makes them excellent candidates for crystal engineering and co-crystal formation.^{1–4} Simple aryl boronic acids tend to form cyclic hydrogen-bonded dimers in the solid state and this motif results in additional hydrogen atoms capable of interacting with guest species. A search of the 2017 version of the Cambridge Structural Database (CSD⁵) reveals some 14 neutral organic co-crystal structure determinations incorporating boric acid itself. Boric acid co-crystals are typically formed with nitrogen bases such as pyridines or imidazoles,^{3, 6, 7} or highly polar oxygen acceptors such as triphenylphosphine oxide.⁸ There are also a number of fascinatingly complex inorganic and ionic boric acid co-crystals such as tetraethylammonium carbonate urea clathrate bis(boric acid) monohydrate.⁹ In addition a large number of co-crystal structures have been reported for boronic acid derivatives, as in the co-crystal of the anti-anxiety drug alprazolam with 4-hydroxyphenylboronic acid.¹⁰ Co-crystallization is of increasing interest in the pharmaceutical industry as a formulation strategy in order to modify the solubility, bioavailability and processing characteristics of active pharmaceutical ingredients.^{11–20} There are also emerging applications of co-crystals in agrochemicals.²¹ As a method of modifying the solid state properties and dissolution characteristics of active ingredients,

co-crystallisation (and the formation of co-amorphous phases^{22, 23}) represents a general strategy and should also be applicable to other industry sectors.^{24, 25}

One key application of boric acid is as a crosslinking agent in the production of viscous gels from guar gum.^{26, 27} Guar is a plant cultivated in warm climates, particularly India and Pakistan. The beans produced from guar are edible, but the gum extracted from them has a range of uses as a thickening and stabilizing agent. Guar is a water-soluble polysaccharide comprised of a linear backbone of (1-4)- β -linked D-mannose units with (1-5)- α -linked D-galactose units randomly attached as side chains, Fig. 1. Guar gum is used extensively in industry for example to reduce ice crystal size in ice cream, improve the texture of cheese, thicken face creams and toothpastes, bind tablets for drug delivery and to improve the wear of paper.²⁸ In the oil industry guar is used to thicken mud to help with drilling, as a surfactant to maintain slurries, as a lubricant and to minimise water loss in certain geological formations.^{29–31}

Figure 1 - Repeat unit of guar gum.²⁷

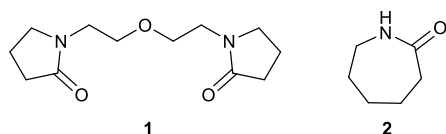
For many applications, especially as a thickening agent, the guar gum is cross-linked. In the presence of water cross-linked guar gum readily swells to form a hydrogel.²⁷ Cross-linking is often performed by borate ions either by using boric acid at high pH or directly from borax. Hydroxyl groups in the guar react reversibly with the borate ions, losing water and forming a guar-borate complex. When this complex reacts with a second chain of guar a crosslink is formed. As the steps to form the crosslinks are reversible this is a dynamically crosslinked

^a Department of Chemistry, Durham University, South Road, Durham DH1 3LE, UK. Email: jon.steed@durham.ac.uk

^b Ashland LLC, 1005 Route 202/206, Bridgewater, NJ 08807, USA. E-mail: omusa@ashland.com

Electronic Supplementary Information (ESI) available: crystallographic information in CIF format has been deposited with the Cambridge Crystallographic Data Centre, deposition numbers CCDC 1568422–1568426. IR spectra, XRPD data and additional crystallographic and rheology data are available as supplementary information, see DOI: 10.1039/x0xx00000x. The underlying research data for this paper is available in accordance with EPSRC open data policy from DOI: 10.15128/r27m01bk681.

system, so the gel can be broken and reformed easily which has important implications on its rheology. New methods of crosslinking are of industrial interest, either to reduce cost, vary the properties of the final product or change the rate of the crosslinking reaction. We now report our initial investigations into slow-release co-crystal forms of boric acid and boric acid derivatives stabilised by lactams **1** and **2** and their application in the guar cross-linking process.³²



Results and Discussion

Bis(pyrrolidone) co-crystals

Reaction of the neutral bis(pyrrolidone) ether 1-{2-[2-(2-oxo-pyrrolid-1-yl)-ethoxy]-ethyl}-pyrrolid-2-one (**1**) with boric acid in a stoichiometric ratio in ethanol, results in the crystallization of a hydrogen-bonded co-crystal of formula $1 \cdot 2\text{B}(\text{OH})_3$. The new material was analysed using single crystal X-ray diffraction and IR spectroscopy. The asymmetric unit, contains a single bis(pyrrolidone) and two boric acid molecules, held by very short $\text{BOH} \cdots \text{O}=\text{C}$ interactions ($\text{O} \cdots \text{O}$ distances 2.658(1) and 2.605(1) Å). Such short contacts are indicative of strong hydrogen bonding as a result of the high polarity of the carbonyl moiety. All three hydroxyl moieties of the boric acid molecule are involved in hydrogen bonding interactions; two OH groups interact with neighbouring boric acid molecules to form a tape arrangement, while the remaining OH group interacts with the carbonyl functionality of a pyrrolidone. This results in hydrogen-bonded ladders of boric acid, with bridging bis-pyrrolidones, Fig. 2.

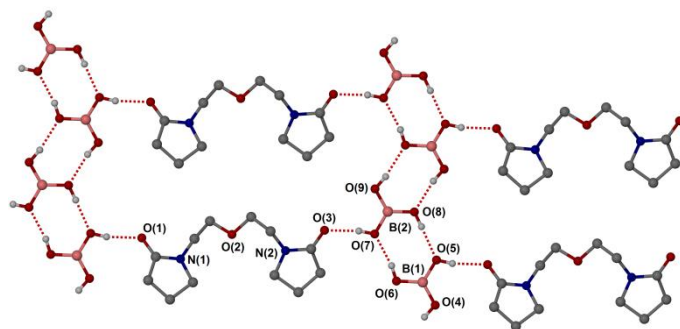


Figure 2. X-ray structure of $1 \cdot 2\text{B}(\text{OH})_3$. CH hydrogen atoms omitted for clarity. Selected hydrogen bonding distances (Å): $\text{O}(6) \cdots \text{O}(7)$ 2.6860(14), $\text{O}(7) \cdots \text{O}(3)$ 2.6045(13), $\text{O}(4) \cdots \text{O}(8)$ 2.7000(14), $\text{O}(9) \cdots \text{O}(6)$ 2.7541(13), $\text{O}(5) \cdots \text{O}(1)$ 2.6583(13), $\text{O}(8) \cdots \text{O}(5)$ 2.7350(14).

In the FTIR spectrum of **1** as a thin film the carbonyl stretching mode occurs at 1674 cm^{-1} , shifting to 1641 cm^{-1} in $1 \cdot 2\text{B}(\text{OH})_3$. This shift is similar to those seen upon hydration and metal complexation of **1** and is indicative of a shift to the enolate resonance form and hence strong hydrogen bonding interactions.^{33, 34}

The co-crystal was also prepared mechanochemically.³⁵ Solvent-free grinding of **1** and boric acid, in a 1:2 ratio using a pestle and mortar, results in the immediate formation of a white paste that transforms to a white crystalline solid upon air drying over a period of 3 hours at room temperature. The IR spectrum of the mechanochemically prepared material is consistent with that for $1 \cdot 2\text{B}(\text{OH})_3$, (supplementary information Fig. S1). The mechanochemical formation of $1 \cdot 2\text{B}(\text{OH})_3$ was also confirmed by XRPD. The crystals adopt an extreme blade-shaped morphology and the experimental XRPD pattern is significantly affected by preferred orientation, however it proved possible to obtain a Rietveld fit to the XRPD data based on the experimental single crystal structure (supplementary information Figs. S2 and S3).

Slow evaporation of a 1:1 molar ratio of **1** and the bifunctional 1,4-phenylenediboric acid in water resulted in a 1:1 co-crystal $1 \cdot \text{C}_6\text{H}_4\text{B}_2(\text{OH})_4$. The single crystal X-ray structure is shown in Fig. 3. The 1,4-phenylenediboric acid molecules form chains with the molecules of **1** bridging between two chains by accepting hydrogen bonds from the boronic acid groups. In the 1,4-phenylenediboric acid chain the torsion angle between the phenylene ring and the boronic acid moiety is $28.35(16)^\circ$ on the side hydrogen bonding to **1** and $10.48(15)^\circ$ on the side hydrogen bonding to the next 1,4-phenylenediboric acid molecule. The hydrogen bonds between the 1,4-phenylenediboric acid molecules have $\text{O} \cdots \text{O}$ distances of 2.810(2) Å and 2.754(2) Å. In comparison, in 1,4-phenylenediboric acid itself³⁶ the $\text{O} \cdots \text{O}$ distances both the same at 2.761(3) Å and the torsion angles at both ends of the 1,4-phenylenediboric acid molecule are much more similar to each other with values of 23.5° and 25.0° . The larger torsion angles are associated with hydrogen bonding from the boronic acid chain to external acceptors (either **1** or other boronic acid groups in the parent compound). In co-crystal $1 \cdot \text{C}_6\text{H}_4\text{B}_2(\text{OH})_4$ there is an unusual double donor/double acceptor geometry of the boronic acid chain as opposed to the usual cyclic donor/acceptor motif. As a result an external hydrogen bond at one end of the motif is not required, resulting in a cyclic hydrogen bonding arrangement that is essentially coplanar with the phenylene ring.

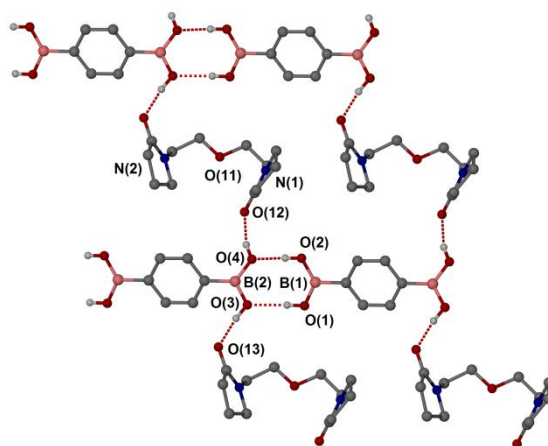


Figure 3. X-ray structure of $1\cdot\text{C}_6\text{H}_4\text{B}_2(\text{OH})_4$. CH hydrogen atoms omitted for clarity. Selected hydrogen bonding distances (Å): O(1)⋯O(3) 2.810(2), O(2)⋯O(4) 2.754(2), O(3)⋯O(13) 2.699(1) and O(4)⋯O(12) 2.626(2).

The hydrogen bonds between **1** and 1,4-phenylenediboric acid molecules have similar O⋯O distances to $1\cdot\text{B}(\text{OH})_3$ (2.626(2) Å and 2.699(1) Å vs. 2.658(1) Å and 2.605(1) Å) again suggesting very strong interactions to the polar lactam carbonyl groups. The conformation of the bis(pyrrolidone) in the two structures is very different, however, consistent with its flexible structure.

Hirshfeld surface analysis is an excellent way to visualise intermolecular interactions in crystals in a holistic way.^{37, 38} The Hirshfeld surface is constructed by partitioning space in the crystal into regions where the electron distribution of a sum of spherical atoms for the molecule dominates the corresponding sum over the crystal. Normalised short contacts from within (d_i) and outside (d_e) the surface can be represented on a fingerprint plot. The Hirshfeld surface fingerprint plots for co-former **1** in $1\cdot\text{C}_6\text{H}_4\text{B}_2(\text{OH})_4$ and $1\cdot 2\text{B}(\text{OH})_3$ are shown in Figure 4. Both plots exhibit a sharp peak at the bottom of the plot (black arrows) characteristic of hydrogen bond accepting behaviour by the lactam carbonyl oxygen atom. However, $1\cdot 2\text{B}(\text{OH})_3$ also exhibits a small peak indicative of hydrogen bond donating behaviour arising from a single C-H⋯O hydrogen bond to the boric acid.

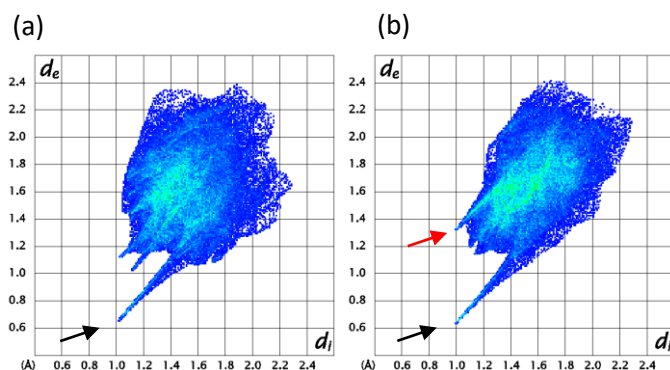


Figure 4. Hirshfeld surface fingerprint plots for co-former **1** in a) $1\cdot\text{C}_6\text{H}_4\text{B}_2(\text{OH})_4$ and b) $1\cdot 2\text{B}(\text{OH})_3$. OH⋯O hydrogen bonds are highlighted by black arrows while the red arrow indicates CH⋯O hydrogen bonding.

The solid state FTIR spectrum of $1\cdot\text{C}_6\text{H}_4\text{B}_2(\text{OH})_4$ showed a carbonyl stretch at 1647 cm^{-1} similar to $1\cdot 2\text{B}(\text{OH})_3$, consistent with the strongly hydrogen bonded structure.

ϵ -Caprolactam co-crystals

While the supramolecular chemistry of compound **1** is dominated by its strong hydrogen bond acceptor ability, ϵ -caprolactam is both a good hydrogen bond acceptor and donor with the seven-membered ring imparting a higher degree of polarity to the carbonyl group than the five-membered ring analogue.³³ Grinding a 1:1 mixture of ϵ -caprolactam (**2**) and boric acid in a ball mill gave a homogeneous powder of a 1:1 co-crystal $2\cdot\text{B}(\text{OH})_3$. The co-crystal was identified by the characteristic hydrogen bonding induced shift in the carbonyl band in the solid state FTIR spectrum of the product (from 1653 to 1623 cm^{-1}) and by its

unique XRPD pattern. A single crystal of the product was serendipitously obtained as a decomposition product from a co-crystallization attempt with a vinylcaprolactam derivative. XRPD established that the single crystal is representative of the bulk mechanochemically produced material (supplementary material, Fig. S5). The boric acid molecules adopt the same chain of cyclic hydrogen bonded motifs as in $1\cdot 2\text{B}(\text{OH})_3$ but the CH⋯O hydrogen bond in the co-crystal with **1** is replaced by a shorter NH⋯O interaction which occupies the remaining acceptor site on the boric acid, Fig. 5. The enhanced hydrogen bond donor ability of **2** is reflected in the Hirshfeld surface fingerprint plot which has a much more distinctive hydrogen bond donor feature (Supplementary information Fig. S6). The crystal adopts an interdigitated layered structure with no significant inter-layer interactions. The boric acid to ϵ -caprolactam hydrogen bonds have a particularly short O⋯O distance of 2.564(1) Å and a rather long N⋯O distance of 3.035(1) Å. In comparison, most similar ϵ -caprolactam to hydroxyl group hydrogen bonds in the CSD exhibit O⋯O distance of around 2.67 Å,^{39, 40} although a sulfonamide benzoic acid/ ϵ -caprolactam co-crystal reported by the Nangia group⁴¹ exhibits a comparable O⋯O interaction between the carbonyl of the ϵ -caprolactam molecule and the hydroxyl group of sulfonamide benzoic acid of length 2.56 Å.

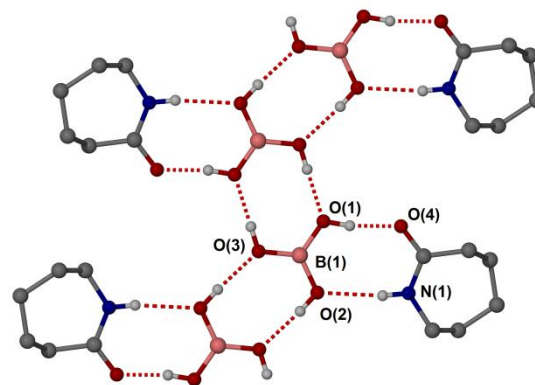


Figure 5. X-ray structure of $2\cdot\text{B}(\text{OH})_3$. CH hydrogen atoms omitted for clarity. Selected hydrogen bonding distances (Å): O(1)⋯O(4) 2.564(1), O(1)⋯O(3) 2.657(1), O(2)⋯O(3) 2.707(1) and N(1)⋯O(2) 3.035(1).

An interesting 2:1 ϵ -caprolactam co-crystal was also isolated as a decomposition product from the 1:1 reaction of *N*-vinyl caprolactam with 4-hydroxyphenylboronic acid in methanol to give $2_2\cdot\text{C}_6\text{H}_4(\text{OH})\text{B}(\text{OH})_2$. The X-ray structure of this co-crystal is shown in Fig. 6 and is based on an unusual $R_3^3(10)$ hydrogen bonded ring graph set⁴² involving two ϵ -caprolactam units and the boronic acid functionality. The structure also incorporates significant CH⋯ π interactions from the caprolactam CH_2 groups that appear as prominent 'wings' in the Hirshfeld surface fingerprint plot (supplementary information, Fig. S7). The X-ray crystal structure of 4-hydroxyphenylboronic acid itself was also determined for comparison and lacks these features. The structure adopts $Z' = 2$ as is relatively common for monoalcohols⁴³ and is consistent with the increased tendency for molecule with a parent structure with high Z' to form co-crystals.⁴⁴ The details of the

structure are given in the supplementary material (Figs. S8 and S9). Unfortunately it proved impossible to prepare the co-crystalline material directly from slow evaporation of mixtures of **2** and 4-hydroxyphenylboronic acid, and instead oily products were obtained. As a result this material was not pursued further.

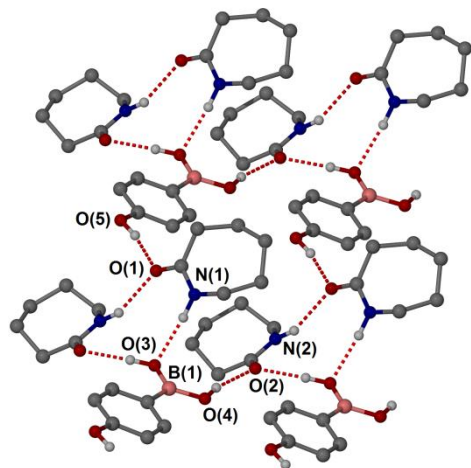


Figure 6. X-ray structure of $2 \cdot C_6H_4(OH)B(OH)_2$. CH hydrogen atoms omitted for clarity. Selected hydrogen bonding distances (Å): N(2)⋯O(1) 2.914(4), N(1)⋯O(3) 2.969, O(3)⋯O(2) 2.803(4), O(4)⋯O(2) 2.733(4), O(5)⋯O(1) 2.664.

Guar gelation

In order to establish whether delivery of the boric acid cross-linker as a co-crystal affects the guar cross-linking process and resulting guar gel characteristics, we studied guar cross-linking by boric acid itself and boric acid co-crystals $1 \cdot 2B(OH)_3$ and $2 \cdot B(OH)_3$. Guar gels were prepared according to the method of Bishop *et al.* using a 10:2000:1 wt/wt/wt ratio of guar:water:boric acid with a small amount of NaOH to raise the pH above 9.⁴⁵ Initial tests focused on a weight-for-weight comparison of $1 \cdot 2B(OH)_3$ and boric acid as cross-linkers. The cross-linker was added at 10 wt% relative to guar to sonicated, homogeneous aqueous guar (5 mg mL⁻¹). After shaking to ensure dissolution 2M sodium hydroxide solution was added dropwise and the solution thoroughly mixed. One pair of samples with either boric acid itself or $1 \cdot 2B(OH)_3$ as cross-linker were then heated with a heat gun and allowed to cool (samples A and B). A second pair was kept at room temperature (samples C and D). Gel formation was assessed by the simple inversion test; strong gels typically hold their shape and do not fall upon sample inversion (See Fig. S12, supplementary information for images of the gels).

As anticipated, the boric acid cross-linked systems (A and C) form viscous gels almost immediately following addition of NaOH. The gels increase in viscosity when left undisturbed for 5 minutes. After 10 minutes, sample C is able to hold the shape of the vial and does not fall upon inversion. Heating of the mixture (as in A) results in increased homogeneity and a quicker transition to the gel state. In comparison, upon addition of NaOH to the co-crystal cross-linked system (sample

D), the mixture appears to thicken slightly but remains reasonably free-flowing and is initially considerably less viscous than boric acid cross-linked system C. The sample viscosity increases upon leaving undisturbed, and after 10 minutes the material holds the shape of the vial and does not fall upon upturning. Analogously to the boric acid control, heating of the mixture results in a quicker transition to the gel state. In both the heated and room temperature systems, the boric acid cross-linker forms a gel more quickly than the systems containing the co-crystal. However, upon leaving undisturbed for approximately 10 minutes the resulting systems are of similar viscosity. The gels appear comparable for 5 days, after which point those containing the co-crystalline species appear to flow more readily. It is interesting that the lower boron-to-polysaccharide molar ratio, in the case of complex $1 \cdot 2B(OH)_2$, still enables formation of a strong gel, albeit at slower rate.

The same guar thickening studies were conducted using boric acid, 1,4-phenylene diboronic acid and complexes $1 \cdot 2B(OH)_3$, $1 \cdot C_6H_4B_2(OH)_4$ and $2 \cdot B(OH)_3$ on an equivalent molar basis. All samples formed self-supporting gels. In contrast, the less soluble tetrahydroxydiboron proved ineffective as a cross-linker. Use of a molar equivalent boron content of the co-crystals resulted in the thickening of the guar mixture, however the resulting gels were initially apparently weaker than when using uncomplexed boric acid. Over time the mixture containing $1 \cdot 2B(OH)_3$ collapsed more readily than the boric acid equivalent. After 3 days the $1 \cdot 2B(OH)_3$ -guar mixture separated into a biphasic mixture with a liquid layer on top and a gel containing unidentified crystalline material in the lower layer (supplementary information, Fig. S10). A significant effect of mixing time prior to base addition was noted in which for all boric acid cross-linked samples the longer the sample was allowed to mix prior to initiation of the cross-linking by sodium hydroxide addition, the faster gelation occurred (supplementary material, Fig. S11). In contrast for 1,4-phenylenediboronic acid or co-crystal $1 \cdot C_6H_4B_2(OH)_4$ gelation occurred in under a minute regardless of time between mixing and NaOH addition. The mixing time may relate to the accessibility of some of the guar functionality, physical entanglement of the chains or a solubility effect.

Oscillatory stress sweep rheology was used to test the relative strength of the guar gels formed with boric acid, 1,4-phenylenediboronic acid and co-crystals $1 \cdot 2B(OH)_3$, $1 \cdot C_6H_4B_2(OH)_4$ and $2 \cdot B(OH)_3$. Oscillatory stress sweeps were performed using a smooth 25 mm steel geometry and 60 mm smooth Peltier steel plate with a gap of 1000 μm. The frequency was fixed at 1 Hz and the stress sweep was performed from 0 – 1000 Pa. The samples for rheology were prepared by mixing water, guar and cross-linker an hour before adding NaOH to avoid any variations arising from mixing time. The samples are shaken to thoroughly mix in the NaOH, which results in air bubbles, which can lead to poorly reproducible rheology results. To ameliorate this problem multiple samples of each gel were measured until reproducible results were obtained. The oscillatory stress sweep rheology for cross-linkers boric acid, $1 \cdot 2B(OH)_3$ and $2 \cdot B(OH)_3$ are shown

in Fig. 7. All three samples are comparable with a storage modulus between 20.9 and 22.6 Pa. The storage modulus for all three samples decreases and eventually crosses over with the loss modulus to give a yield stress of between 225 and 283 Pa, *i.e.* the same as one another within experimental error.

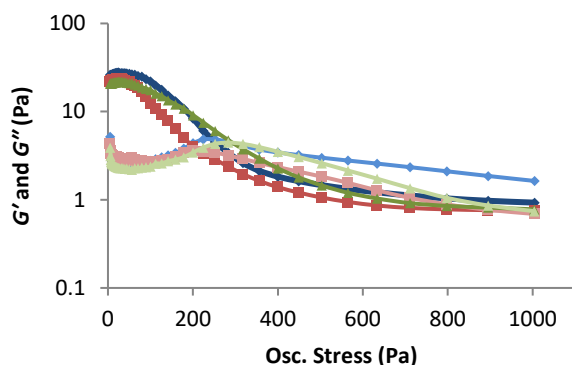


Figure 7. Oscillatory stress sweep rheometry for guar gels crosslinked by boric acid (♦) $1\cdot 2\text{B}(\text{OH})_3$ (■) and $1\cdot \text{C}_6\text{H}_4\text{B}_2(\text{OH})_4$ (▲).

Co-crystal $1\cdot \text{C}_6\text{H}_4\text{B}_2(\text{OH})_4$ and 1,4-phenylenediboronic acid also show similar behaviour to one another. The oscillatory stress sweep, 8, shows both gels have an initial storage modulus of 27 Pa and G' then decreases, with a yield stress of approximately 565 Pa. Interestingly, the 1,4-phenylene diboronic acid gels are consistently stronger than the boric acid gels.

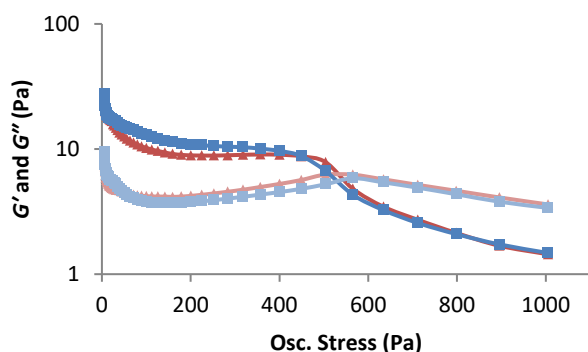


Figure 8. Oscillatory stress sweep rheometry for guar gels crosslinked by 1,4-phenylenediboronic acid (▲) and $1\cdot \text{C}_6\text{H}_4\text{B}_2(\text{OH})_4$ (■).

Conclusions

The high polarity of the amide carbonyl functionality enables formation of co-crystalline species with boric acid and its derivatives. The short hydrogen bond distances between the bis(pyrrolidone) ether and boric acid confirm the strong interactions. The co-crystalline material successfully acts as a cross-linker and boronic acid source upon addition of NaOH. On a weight-for-weight basis the immediately resulting gel is weaker than the analogous boric acid system, however upon leaving to stand for a short time the materials are comparable. On a molar equivalent basis gels formed by co-crystal boron sources behave similarly to the conventional materials. It is

interesting that on a weight basis the lower boron-to-polysaccharide ratio in the co-crystal still enables gel formation. The co-crystal approach to active ingredient delivery in this type of application is a novel one and merits further investigation in terms of co-crystal solubility and delayed release characteristics.

Experimental

General

1-{2-[2-(2-oxo-pyrrolidin-1-yl)-ethoxy]-ethyl}-pyrrolidin-2-one (**1**) was supplied by Ashland LLC.³² 1,4-Phenylenediboronic acid and 4-hydroxyphenylboronic acid was purchased from TCI and used without further purification. All other solvents and reagents were obtained from standard commercial sources. IR spectra were measured with a Perkin-Elmer 100 FT-IR spectrometer, using an ATR attachment. Crystals suitable for single crystal X-ray diffraction structure determination were selected, soaked in perfluoropolyether oil and mounted on a MiTeGen loop. Single crystal X-ray data were collected at 120 K on an Agilent Gemini S-Ultra (Sapphire-3 CCD detector) or Bruker SMART CCD 6000 (compound $1\cdot \text{C}_6\text{H}_4\text{B}_2(\text{OH})_4$) diffractometers equipped with the Cryostream (Oxford Cryosystems) open-flow nitrogen cryostats, using graphite monochromated MoK α -radiation ($\lambda = 0.71073 \text{ \AA}$). The data for $2\cdot \text{B}(\text{OH})_3$ were collected on a Bruker D8 Venture diffractometer (PHOTON100 CMOS detector, pfocusing mirrors, μS Mo-microsource). All structures were solved using direct methods and refined by full-matrix least squares on F^2 for all data using SHELXL⁴⁶ and OLEX2⁴⁷ or X-Seel.⁴⁸ All non-hydrogen atoms were refined with anisotropic displacement parameters. CH hydrogen atoms were placed in calculated positions, assigned an isotropic displacement factor that is a multiple of the parent carbon atom and allowed to ride. H-atoms attached to oxygen atoms were located on the difference map when possible, or placed in calculated positions. X-ray Powder diffraction was performed on glass slides using a Bruker AXS D8 Advance diffractometer, with a Lynxeye Soller PSD Detector, using CuK α radiation at a wavelength of 1.5406 \AA .

Synthesis of co-crystals

$1\cdot 2\text{B}(\text{OH})_3$

1-{2-[2-(2-oxo-pyrrolidin-1-yl)-ethoxy]-ethyl}-pyrrolidin-2-one (**1**) (0.100 g, 0.416 mmol) was added to a solution of boric acid (0.0257 g, 0.416 mmol) in ethanol. The mixture was sonicated to ensure thorough mixing. Slow evaporation at room temperature resulted in single crystals of $1\cdot 2\text{B}(\text{OH})_3$. (Yield = 0.056 g, 0.154 mmol, 37%). The material is also conveniently prepared in essentially quantitative yield by grinding a 1:1 mixture of **1** and boric acid in a mortar and pestle for one minute. Any excess liquid **1** was removed by pressing the mixture between dry filter paper to give an off white solid. FTIR (ν/cm^{-1}) 1641 (C=O) and 1110 (C-O). *Crystal data*: $2(\text{BH}_3\text{O}_3) \cdot \text{C}_{12}\text{H}_{20}\text{N}_2\text{O}_3$, $M = 363.97$, triclinic, space group P-1, $a = 7.0629(4)$, $b = 7.9863(4)$, $c = 17.6846(9) \text{ \AA}$, $\alpha = 79.301(5)^\circ$, $\beta =$

80.217(5)°, $\gamma = 68.622(5)^\circ$, $V = 907.03(8) \text{ \AA}^3$, $Z = 2$, $D_c = 1.333 \text{ g/cm}^3$, $F_{000} = 388$, $\mu = 0.110 \text{ mm}^{-1}$, 10266 reflections collected, 3945 unique ($R_{\text{int}} = 0.0357$). Final GooF = 1.029, $R_1 = 0.0397$ (3067 reflections with $I > 2\sigma(I)$), $wR_2 = 0.0965$ (all data).

1·C₆H₄B₂(OH)₄

1,4-phenylenediboronic acid (0.021 g, 0.124 mmol) and compound **1** (0.045 g, 0.188 mmol) were dissolved in water and the solution allowed to evaporate at room temperature. Crystals of diffraction quality formed within three weeks and analysed by single crystal x-ray crystallography. A second sample was prepared by grinding a 1:1 mixture of **1** and 1,4-phenylenediboronic acid in a mortar and pestle for one minute. FTIR (ν/cm^{-1}) 1647 (C=O). *Crystal data*: C₆H₈B₂O₄·C₁₂H₂₀N₂O₃, $M = 406.04$, triclinic, space group P-1, $a = 10.0731(4)$, $b = 10.2343(4)$, $c = 12.1312(5) \text{ \AA}$, $\alpha = 112.5470(10)^\circ$, $\beta = 111.5550(10)^\circ$, $\gamma = 90.5390(10)^\circ$, $V = 1038.42(7) \text{ \AA}^3$, $Z = 2$, $F(000) = 432.0$, $\mu = 0.097 \text{ mm}^{-1}$, 18453 reflections collected, 6065 unique ($R_{\text{int}} = 0.033$). Final GooF = 1.064, $R_1 = 0.0684$ (4790 reflections with $I \geq 2\sigma(I)$), $wR_2 = 0.1682$ (all data).

2·B(OH)₃

The title compound was prepared by grinding a 1:1 mixture of ϵ -caprolactam and boric acid in a Retsch MM200 ball mill at 20 Hz for 30 min. Single crystals for X-ray diffraction were obtained as a byproduct from the reaction of tetrahydroxydiboron (0.008 g, 0.089 mmol) 1,3-bis(2'-caprolactam-1'-yl)but-1-ene⁴⁹ (0.04 g, 0.14 mmol) together in water and allowing the water to evaporate at room temperature. Single crystals of diffraction quality were analysed after three weeks. *Crystal data*: C₆H₁₁NO·B(OH)₃, $M = 174.99$, monoclinic, space group $P2_1/n$, $a = 6.9008(3)$, $b = 18.7679(8)$, $c = 7.4385(3) \text{ \AA}$, $\beta = 111.3340(10)^\circ$, $V = 897.37(7) \text{ \AA}^3$, $Z = 4$, $F(000) = 376.0$, $\mu = 0.104 \text{ mm}^{-1}$, 19366 reflections collected, 2628 unique ($R_{\text{int}} = 0.0310$). Final GooF = data = 2628, parameters = 165, goodness-of 1.056, $R_1 = 0.0436$ (2218 reflections with $I > 2\sigma(I)$), $wR_2 = 0.0903$ (all data).

2·C₆H₄(OH)B(OH)₂

Vinyl caprolactam (0.0300 g, 0.216 mmol) was added to a solution of 4-hydroxyphenylboronic acid (0.0300 g, 0.216 mmol, TCI Chemicals) dissolved in MeOH. The mixture was sonicated to ensure thorough mixing. Slow evaporation at room temperature resulted in single crystals of the title compound as a degradation product after 5 days. (Yield = 0.048 g); IR (ν/cm^{-1}) 1647 (C=O). *Crystal data*: C₆H₇BO₃ · 2(C₆H₁₁NO), $M = 364.24$, monoclinic, space group $P2_1/n$, $a = 6.4207(3)$, $b = 26.1612(11)$, $c = 11.4892(4) \text{ \AA}$, $\beta = 93.522(4)^\circ$, $V = 1926.22(14) \text{ \AA}^3$, $Z = 4$, $D_c = 1.256 \text{ g/cm}^3$, $F_{000} = 784$, $\mu = 0.090 \text{ mm}^{-1}$, 28141 reflections collected, 3771 unique ($R_{\text{int}} = 0.1271$). Final GooF = 0.906, $R_1 = 0.0594$ (2422 reflections with $I > 2\sigma(I)$), $wR_2 = 0.1473$ (all data).

Samples for rheology were prepared by dissolving guar (0.01 g) and either boric acid (0.001 g), 1,4-phenylenediboronic acid (0.0027 g), or co-crystals 1·2B(OH)₃ (0.0024 g), 1·C₆H₄B₂(OH)₄

(0.0065 g) or 2·B(OH)₃ (0.0045 g) in water (2 mL), shaking for 30 seconds followed by 30 seconds of sonication. After one hour 0.1 cm³ of 2M NaOH was added and the samples were vigorously shaken for a further 20 seconds. Oscillatory stress sweep experiments were performed on a TA Discovery HR-2 hybrid rheometer equipped with a smooth 25 mm steel geometry and 60 mm smooth Peltier steel plate. The gel was positioned on the steel plate below the geometry using a spatula. The geometry was lowered to a distance 1000 μm from the plate. The frequency was set at 1 Hz and the stress sweep was performed from 0.1 - 1000 Pa at 25 °C. Data was recorded using TRIOS v4.1.0.31739.

Acknowledgements

We thank the Engineering and Physical Sciences Research Council for funding via the Doctoral Training Partnership and Ashland LLC for studentship funding. We are also grateful to Prof. J. S. O. Evans and Mr. G. Oswald (Durham University) for help with the XRPD data.

Notes and references

- R. Nishiyabu, Y. Kubo, T. D. James and J. S. Fossey, *Chem. Commun.*, 2011, **47**, 1124.
- J. H. Fournier, T. Maris, J. D. Wuest, W. Z. Guo and E. Galoppini, *J. Am. Chem. Soc.*, 2003, **125**, 1002.
- A. Vega, M. Zarate, H. Tlahuext and H. Hopfl, *Acta Crystallogr. Sect. C*, 2010, **66**, O219.
- S. E. Kutyla, D. K. Stepien, K. N. Jarzemska, R. Kaminski, L. Dobrzycki, A. Ciesielski, R. Boese, J. Mlochowski and M. K. Cyranski, *Cryst. Growth Des.*, 2016, **16**, 7037.
- C. R. Groom and F. H. Allen, *Angew. Chem., Int. Ed.*, 2014, **53**, 662.
- A. Mirjafari, L. Pham, P. J. Smith, R. E. Sykora and J. H. Davis, Jr, *Acta Crystallogr. Sect. E*, 2013, **69**, o1067.
- L. E. Cheruzel, M. S. Mashuta and R. M. Buchanan, *Chem. Commun.*, 2005, 2223.
- A. N. Chekhlov, *Russ. J. Inorg. Chem.*, 2005, **50**, 1298.
- Q. Li, F. Xue and T. C. W. Mak, *Inorg. Chem.*, 1999, **38**, 4142.
- S. Varughese, Y. Azim and G. R. Desiraju, *J. Pharm. Sci.*, 2010, **99**, 3743.
- N. J. Babu and A. Nangia, *Cryst. Growth Des.*, 2011, **11**, 2662.
- H. G. Brittain, *Cryst. Growth Des.*, 2011, **12**, 1046.
- N. Qiao, M. Li, W. Schlindwein, N. Malek, A. Davies and G. Trappitt, *Int. J. Pharm.*, 2011, **419**, 1.
- Ö. Almarsson, M. L. Peterson and M. Zaworotko, *Pharm. Patent Anal.*, 2012, **1**, 313.
- M. Baldrighi, G. Cavallo, M. R. Chierotti, R. Gobetto, P. Metrangolo, T. Pilati, G. Resnati and G. Terraneo, *Mol. Pharm.*, 2013, **10**, 1760.
- S. Aitipamula, P. S. Chow and R. B. H. Tan, *CrystEngComm*, 2014, **16**, 3451.
- K. M. Steed and J. W. Steed, *Chem. Rev.*, 2015, **115**, 2895.
- E. Grothe, H. Meekes, E. Vlieg, J. H. ter Horst and R. de Gelder, *Cryst. Growth Des.*, 2016, **16**, 3237.
- N. Blagden, S. J. Coles and D. J. Berry, *CrystEngComm*, 2014, **16**, 5753.
- D. J. Berry and J. W. Steed, *Adv. Drug Deliv. Rev.*, 2017, **117**, 3.
- Patent WO 2013030777, 2013.
- K. Löbmann, R. Laitinen, H. Grohgan, K. C. Gordon, C. Strachan and T. Rades, *Mol. Pharm.*, 2011, **8**, 1919.
- P. A. Corner, J. J. Harburn, J. W. Steed, J. F. McCabe and D. J. Berry, *Chem. Commun.*, 2016, **52**, 6537.
- C. B. Aakeroy, T. K. Wijethunga, J. Benton and J. Desper, *Chem. Commun.*, 2015, **51**, 2425.
- C. B. Aakeroy, T. K. Wijethunga and J. Desper, *Chem.-Eur. J.*, 2015, **21**, 11029.
- https://en.wikipedia.org/wiki/Guar_gum, (accessed 4/8/17).
- S. Kesavan and R. K. Prud'homme, *Macromolecules*, 1992, **25**, 2026.
- R. J. Chudzinkowski, *J. Soc. Cosmet. Chem.*, 1971, **22**, 43.
- V. Mahto and V. P. Sharma, *J. Petroleum Sci. Eng.*, 2004, **45**, 123.
- US Pat., 6620769, 2003.
- US Pat., 5646093, 1990.
- US Pat., 2012/0148514 A1, 2012.
- A. Perrin, M. J. Goodwin, O. M. Musa, D. J. Berry, P. Corner, K. Edkins, D. S. Yufit and J. W. Steed, *Cryst. Growth Des.*, 2017, **17**, 3236.

34. A. Perrin, D. Myers, K. Fucke, O. M. Musa and J. W. Steed, *Dalton Trans.*, 2014, **43**, 3153.
35. S. L. James, C. J. Adams, C. Bolm, D. Braga, P. Collier, T. Friscic, F. Grepioni, K. D. M. Harris, G. Hyett, W. Jones, A. Krebs, J. Mack, L. Maini, A. G. Orpen, I. P. Parkin, W. C. Shearouse, J. W. Steed and D. C. Waddell, *Chem. Soc. Rev.*, 2012, **41**, 413.
36. P. Rodriguez-Cuamatzi, G. Vargas-Diaz, T. Maris, J. D. Wuest and H. Hopfl, *Acta Crystallogr. Sect. E.*, 2004, **60**, O1316.
37. M. A. Spackman and D. Jayatilaka, *CrystEngComm*, 2009, **11**, 19.
38. P. A. Wood, J. J. McKinnon, S. Parsons, E. Pidcock and M. A. Spackman, *CrystEngComm*, 2008, **10**, 368.
39. J. A. Bis, O. L. McLaughlin, P. Vishweshwar and M. J. Zaworotko, *Cryst. Growth Des.*, 2006, **6**, 2648.
40. P. Sanphui, G. Bolla, A. Nangia and V. Chernyshev, *IUCrJ*, 2014, **1**, 136.
41. G. Bolla and A. Nangia, *Chem. Commun.*, 2015, **51**, 15578.
42. J. Bernstein, R. E. Davis, L. Shimoni and N.-L. Chang, *Angew. Chem. Int. Ed. Engl.*, 1995, **34**, 1555.
43. C. P. Brock and L. L. Duncan, *Chem. Mater.*, 1994, **6**, 1307.
44. K. M. Anderson, M. R. Probert, C. N. Whiteley, A. M. Rowland, A. E. Goeta and J. W. Steed, *Cryst. Growth. Des.*, 2009, **9**, 1082.
45. M. Bishop, N. Shahid, J. Z. Yang and A. R. Barron, *Dalton Trans.*, 2004, 2621.
46. G. M. Sheldrick, *Acta Crystallogr. Sect. A*, 2008, **64**, 112.
47. O. V. Dolomanov, L. J. Bourhis, R. J. Gildea, J. A. K. Howard and H. Puschmann, *J. Appl. Crystallogr.*, 2009, **42**, 339.
48. L. J. Barbour, *J. Supramol. Chem.*, 2001, **1**, 189.
49. J. R. Davenport, O. M. Musa, M. J. Paterson, M. O. M. Piepenbrock, K. Fucke and J. W. Steed, *Chem. Commun.*, 2011, **47**, 9891.

For Table of Contents use only

Boric acid / lactam co-crystals have been applied as novel delivery agents for guar cross-linking

